Arab J Geosci (2014) 7:3251–3257
DOI 10.1007/s12517-013-0920-7

ORIGINAL PAPER

# Experimental creep tests and prediction of long-term creep behavior of grouting material

**Siavash Nadimi · Koroush Shahriar**

Received: 30 April 2012 / Accepted: 15 March 2013 / Published online: 24 April 2013


**Abstract** Rock reinforcement systems, such as resin-grouted rock bolts, display complex creep behavior because both grouting materials and bolts show time-dependent behavior. In this paper, only the time-dependent behavior of grouting material was investigated, in which creep tests of grouting material was conducted in triaxial compression apparatus at room temperature. The test specimens were provided from the Araldite epoxy resin used in rock reinforcement. We attempt to predict long-term creep parameter using triaxial creep tests and to define time-dependent characteristics of the bounding material. In short-term creep tests, three different axial and confining stress levels were applied in steps to each specimen. The transient creep for all the stress levels were described by power function which fit properly to time–strain curves. The maximum difference between the proposed model and experimental long-term creep strain was less than 7.1 %. It was observed that the creep rate of a grouting material specimen directly depends on the deviator of stress (i.e., $\sigma_1$–$\sigma_3$).

**Keywords** Reinforcement system · Triaxial · Araldite epoxy · Power function · Creep

S. Nadimi (✉) · K. Shahriar
Mining and Metallurgical Engineering,
Amirkabir University of Technology, Tehran, Iran
e-mail: nadimisiavash@Gmail.com

S. Nadimi
e-mail: nadimi@aut.ac.ir

K. Shahriar
e-mail: k.shahriar@aut.ac.ir

## Introduction

The understanding of time-dependent effects or creep behavior is important for further development of knowledge in the field of rock mechanics, support system, ground control, and other geological and geophysical phenomena (Lama and Vutukuri 1978; LeComte 1965; Barla 2001; Zhang et al. 2006; Zarei and Sharifzadeh 2010). An increase of pressure on support system due to creep behavior of rock is one of the most important issues in underground structure with weak surrounding rock mass (Nadimi et al. 2010; Ghorbani and Sharifzadeh 2009; Boidy et al. 2002; Soleiman et al. 2011).

The properties of grouting materials have a great effect on stability of grouting rock bolts and it plays a significant role in the selection of bolt type; therefore, the characteristic of grouting material should be investigated for analyzing the stability of supported underground structures (Hobst and Zajíc 1983).

Although, several studies have investigated effects of stress ratio and confining stress (i.e., $\sigma_1$–$\sigma_3$) on creep rate of rock specimens (Kranz 1980; Yongsheng and Changrong 2005; Lockner and Byerlee 1977; Atkinson 1975; Heap et al. 2008), the most uncertain and most difficult aspect of the reinforcement system is predicting of time-dependent behavior of grouting resin. The phenomenon of creep is still far from being fully understood (Mollamahmutoglu 1999; Byung et al. 2007).

The grouting material exhibits a far more complex time-dependent behavior than normal Portland concrete (Charalambous 1991). Its strength and stiffness change with time, and they are strongly influenced by differential stress ($\sigma_1$–$\sigma_3$) in supporting systems. However, realistic prediction of grouting resin creep is of great importance for durability and long-term serviceability of reinforcement systems. Short-term creep tests were carried on

grouting resin to achieve good long-term prediction of creep.

## Test descriptions

Creep studies were carried out on cylindrical specimen of grouting material under triaxial compressive stresses. The cylindrical samples of 75 mm diameter were gained from casting grouting material for a month age in rock mechanics laboratory. The specimens had the ratio of length to diameter of 2–2.2 to approximately meet American Society for Testing and Materials (ASTM) D 4543 (ASTM D 4543 (Reapproved 1991)) and tests were conducted in triaxial compression apparatus at room temperature.

In the paper, Araldite epoxy resin was used for studying the time-dependent behavior. It is a very fast setting, high performance, and non-shrink cementitious grout, manufactured from cement and a special blend of modifiers. The resultant thixotropic grout is well suited as a pumpable grout for use with bolts, cable bolt, gas drainage pipes, and consolidation of broken strata by injection (Celtite catalogue). The ultimate compressive strength (UCS) tests were conducted on the grouting material, and then the same grouting was used for conducting creep tests. The mechanical properties of the grout material are presented in Table 1

The test apparatus has a cell and sample holder where the sample was set in the cell, and it was loaded axially and radially (laterally). Two LVDTs systems were used to measure radical deformation of samples, and they connected to a digital readout device to read the displacements. For applying a steady and an uninterrupted load to specimens, a hydropneumatic accumulator was used. The accumulators have been used as a pressure stabilizer, and consist of specially designed reservoir, which can work under high-pressure gas (Oil Air Hydraulics Inc. catalogue).

## Experiments

There are no standard tests that are directly applicable to grouting materials; therefore, ASTM standards developed for cement were adopted as guidelines. In short-term creep test, the grouting resin cylinder specimens were tested in triaxial compression using hydraulic-loaded creep rig. Constant axial stress ratios (i.e., 60, 70, and 80 %) of UCS were applied to the specimens. The axial stress levels, after decreasing strain, were increased in three steps. Several specimens were tested under three constant confining stress of 0, 5, and 8 MPa.

**Table 1** Mechanical properties of the grout material

| | |
|---|---|
| Water per 20-kg bag | 8 l |
| Age (h) 48 | Compressive strength (MPa): 38.3 |
| Setting time | 90 min |
| Fresh wet density | 2.09 |
| Working life | 30 min |

### Multiple stress levels test

It is obvious that for grouting materials with variability in time-dependent behavior, defining the ultimate long-term strength under different loading condition is very hard. It is difficult to complete a creep test with a single stress level within a month, because it is difficult to select a stress level which assuredly clarifies time-dependent behavior of materials without instantaneously leading to failure. Therefore several multiple stress level creep tests were conducted for understanding time-dependent behavior of the grouting material. The longest test lasted more than 9,500 h (more than 1 year). Figure 1 gives the complete axial strain–time curves for three tests, in which compressive normal stresses and longitudinal strains are positive.

Power and exponential functions have been checked by curve fitting to the multiple stress levels test of creep data. Axial strain–time plots and fitting curves for tests LTC01, LTC02, and LTC03 are found in Fig. 2. Therefore, the power function was chosen for investigating the time-dependent behavior of the grouting material, because the power function fit properly to time–strain curves and also the time-dependent parameters can easily gain from the curves to investigate the time-dependent behavior of the grouting material. As soon as the axial is increased, the axial strain increased as power function of time. Approximately, all of the curves show transient creep behavior. All of the axial strain–time plots adjusted to zero intercept see Fig. 2. The power function in Eq. (1) gives a

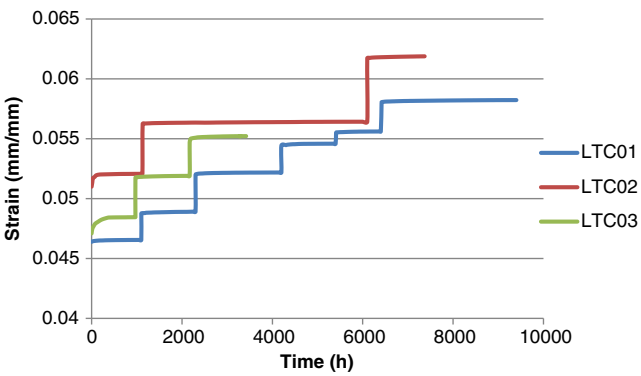


**Fig. 1** Axial strain–time curves for the three multiple stress level tests

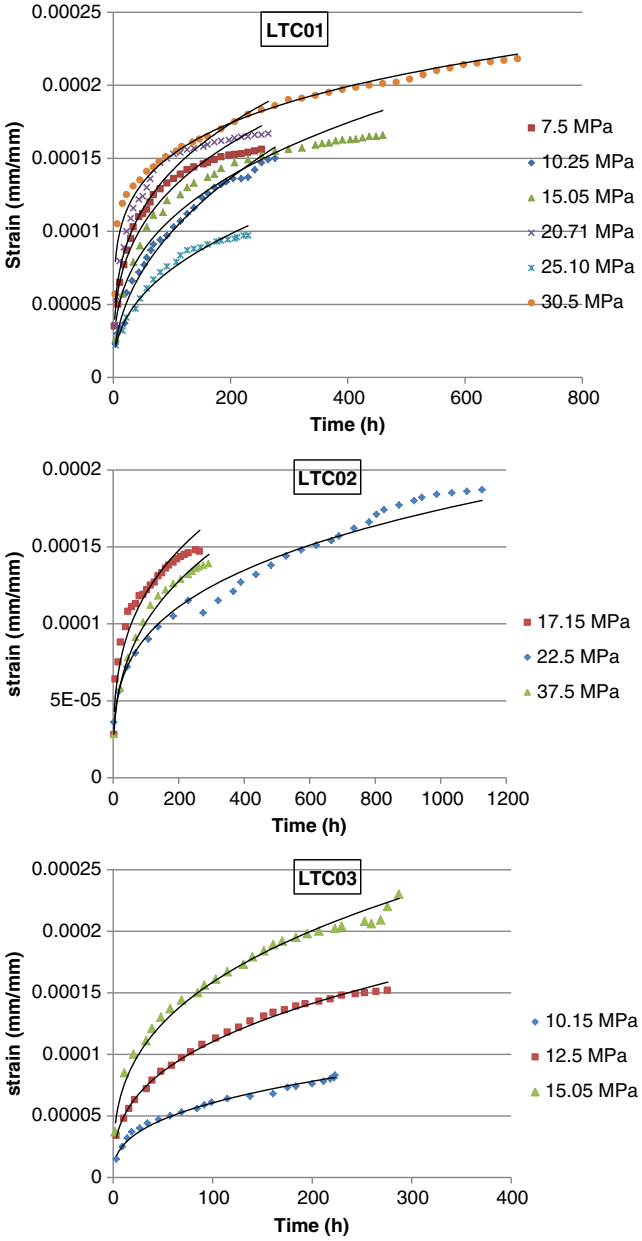


**Fig 2** Experimental axial strain–time plots for transient creep and fitting curves at stress levels given in inserts

significantly better fit. This agrees with Cruden (Cruden 1971; Ping and Xilun 1996).

$$\varepsilon_{tr} = \varepsilon_0 + \alpha t^{\beta} \tag{1}$$

Where $\varepsilon_0$ is the initial axial strain, and $\alpha$ and $\beta$ are material constants. The equations for the curves were estimated using nonlinear regressions in the Excel SOLVER of Microsoft Office 2007. The constants $\alpha$ and $\beta$ in each equation were estimated by maximizing the pseudo-$R^2$, the ratio of the regression sum of squares to the total sum of squares. This ratio explains the proportion of variance accounted for in the dependent variable by the model. It is equivalent to the $R^2$, the coefficient of determining, in linear regression. The values of $\alpha$, $\beta$, and pseudo-$R^2$ in all the equations are listed in Table 2.

All of the pseudo-$R^2$ s values are high, which indicates that all the curves fit the experimental plots well. By taking the derivative of Eq. (1) with respect to time ($t$), the strain rate for the transient creep is obtained as

$$\dot{\varepsilon}_{tr} = \alpha \times \beta \times t^{\beta-1} \tag{2}$$

Equation (2) takes the same from as the empirical low for rock salt proposed by quoted by Jaeger and Cook (1979), and proposed by Dusseault and Fordham (1993) for transient creep. In Andrade's, study the exponent of $t$ was −2/3. Our exponent of $t$ is calculated based on the values of $\beta$ in Table 5. We obtained the mean −0.67 with a standard deviation 0.07. The transient creep is essentially caused by the elastic aftereffect of the specimen. The elastic is due to the thermoelastic property of the specimen.

## Prediction method

There are many ways to describe the time-dependent behavior of materials. One of the best ways to achieve good long-term prediction is the using of short-term creep test (multiple stress levels test) on the given grouting resin, and then by using Bayesian statistics extrapolates the results (Wawersik and Zimmerer 1994). A long-term creep strain curve was constructed using the creep strain curves of short-term creep tests performed at different axial and confining stress levels.

Based on the time–stress analogy, a prediction was conducted by using the results of short-term creep tests which are performed at 21.1, 24.6, and 28 MPa stress levels to predict the long-term creep strain at 21.1 MPa stress level. Therefore, three multiple stress creep tests were conducted on three specimens and each level creep tests lasted for 48 h. It is worth mentioning that the method could be used for predicting time-dependent behavior in any stress level.

This method takes the instantaneous elastic strain, measured at $t$=0 h or during the initial time of applying pressure, and the 48-h creep strain values of each short-term creep test to develop a Prony series (Chen 2000) equation for the long-term creep strain.

**Table 2** Values of $\alpha$, $\beta$, and pseudo-$R^2$ for the fitting curves in Fig. 2

| samples | $\alpha$ | $\beta$ | Pseudo-$R^2$ |
|---|---|---|---|
| LTC01 | 53,811 | 0.002 | 0.912 |
| LTC02 | 53,534 | 0.002 | 0.910 |
| LTC03 | 53,326 | 0.001 | 0.012 |

The creep strain values at $t$=0 h and $t$=48 h are used to determine the coefficient of the following Prony series equation:

$$\varepsilon(t) = \varepsilon_e + D_1\left(1 - e^{\frac{-t}{\tau_1}}\right) \tag{3}$$

Where $\varepsilon_e$ is the instantaneous elastic strain, which is measured at $t$=0 h or during the initial time of applying pressure. The retardation time $\tau_1$ is set to time coordinate $t$= 48 h. The 48-h creep strain $\varepsilon(t = 48)$ is substituted in Eq. (3) and the coefficient $D_1$ is determined:

$$D_1 = 1.582[\varepsilon(48) - \varepsilon_e\,] \tag{4}$$

Equation (5) is taken to determine the coefficient $D_1$ for each stress levels. Coefficient $D_1$is then substituted in Eq. (5) in order to develop a Prony series expression for each short-term creep strain curve.

$$\varepsilon^{21.1}(t) = \varepsilon_e^{21.1} + D_1^{21.1}\left(1 - e^{\frac{-t}{48}}\right) \tag{5}$$

$$\varepsilon^{24.6}(t) = \varepsilon_e^{24.6} + D_1^{24.6}\left(1 - e^{\frac{-t}{48}}\right) \tag{6}$$

$$\varepsilon^{28}(t) = \varepsilon_e^{28} + D_1^{28}\left(1 - e^{\frac{-t}{48}}\right) \tag{7}$$

The superscripts 21.1, 24.6, and 28 indicate the axial stress of the short-time creep strain curve that each equation represents. Eqs. (5–7) are then used to develop the following expression for predicting long-term creep strain at 15 MPa:

$$\varepsilon(t) = \varepsilon^{21.1}(t) + \varepsilon_{pred}(t) \tag{8}$$

Where $\varepsilon^{21.1}$ ($t$)is given by Eq. (5). The prediction term $\varepsilon_{pred}$ ($t$) in Eq. (8) is formed from two exponential terms:

$$\varepsilon_{pred}(t) = D_2\left(1 - e^{\frac{-t}{\tau_2}}\right) + D_3\left(1 - e^{\frac{-t}{\tau_3}}\right) \tag{9}$$

Where $\tau_2$ and $\tau_3$ are set at 400 and 4,000 respectively. The values of exponential term $e^{\frac{-t}{\tau}}$ become zero when $t$ increased above $4\tau$. The retardation constants $\tau_2$ and $\tau_3$ therefore have to be large enough as that the exponential terms of Eq. (9) would have effectively nonzero contribution to the long-term creep strain predicted by Eq. (8) (Byung et al. 2007).

It was observed that the coefficient of exponential terms in Eq. (5–7) increased with the axial stress. According to time–stress correspondence, increase in the value of the coefficient, i.e., an increase in the creep strain, could have been caused either by stress or a time increase. The coefficient of the long-term 21.1 MPa curve, $D_2$ and $D_3$, are therefore expressed in terms of the coefficients of the 24.6 and the 28 MPa curve, respectively, by the following expressions:

$$D_2 = r\varepsilon_1^{21.1} \tag{10}$$

$$D_3 = r\varepsilon_1^{28} \tag{11}$$

Where $r$ is the factor used to adjust the coefficients to minimize the error in the predicted creep strain (Charalambous 1991). Knowing how to determine the parameter $r$ is discussed below along with the presentation of the results.

Equations (5) and (9–11) are substituted into Eq. (8) in order to develop the following equation that predicts the long-term creep strain:

$$D(t) = \varepsilon_e^{21.1} + D_1^{21.1}\left(1 - e^{\frac{-t}{48}}\right) + rD_1^{24.6}\left(1 - e^{\frac{-t}{400}}\right) + rD_1^{28}\left(1 - e^{\frac{-t}{4000}}\right) \tag{12}$$

Where the coefficient $D_1^{21.1}$, $D_1^{24.6}$, and $D_1^{28}$ are determined by Eq. (5). Equation (12) can predict the creep strain values for times that do not exceed four times larger retardation time, 4,000 h. the predicted creep strain value remains unchanged as time increase above 1,600 h. For predicting more than 1,600 h we can increase the values of $\tau_2$ and $\tau_3$, but we should pay attention to select these values in a way that not to increase the prediction error.

## Results and discussion

### Prediction of long-term creep behavior

The short-term creep test provided 48-h creep strain values at 21.1, 24.6, and 28 MPa to construct a Prony series equation by which it is possible to predict the long-term creep strain at 21.1 MPa stress level. The proposed method of short-term creep tests was used to predict the long-term creep strain of the grouting resin, incorporating axial and confining stress. Each creep strain curve is representing by the following Prony series at equation:

$$\varepsilon(t) = \varepsilon_e + D_1\left(1 - e^{\frac{-t}{48}}\right) \tag{13}$$

Where $\varepsilon_e$, instantaneous elastic strain, is the creep strain at $t$=0 h (during the initial time of applying pressure). The coefficient $D_1$, which is a function of the instantaneous elastic strain $\varepsilon_e$, and the 48-h creep strain $\varepsilon$ (48) are determined by Eq. (13). The values of the Prony series coefficient$D_1$, for compressive short-term creep tests performed on each sample are shown in Table 3. The 48-h creep factor, $f$ (48), that is the ratio of the specific creep $\varepsilon$

**Table 3** Results of short-term creep test

| Sample | $\sigma_3$ MPa | $\sigma_1$ MPa | $\varepsilon_e$ (μ) | $\varepsilon$ (48) (μ) | $D_1$ (μ) | $f$ (48) |
|---|---|---|---|---|---|---|
| A | | | | | | |
| | 0 | 21.1 | 53,797 | 54,257 | 248.37 | .0029 |
| | 0 | 24.6 | 55,094 | 55,257 | 257.86 | .0029 |
| | 0 | 28 | 56,220 | 56,386 | 278.43 | .0031 |
| B | | | | | | |
| | 5 | 21.1 | 53,541 | 53,664 | 194.58 | .002 |
| | 5 | 24.6 | 54,811 | 54,944 | 210.40 | .0027 |
| | 5 | 28 | 55,880 | 56,023 | 226.22 | .0029 |
| C | | | | | | |
| | 8 | 21.1 | 53,402 | 53,492 | 142.38 | .0016 |
| | 8 | 24.6 | 54,720 | 54,815 | 150.29 | .0017 |
| | 8 | 28 | 55,812 | 55,910 | 155.03 | .0017 |

$(48) - \varepsilon_e$ to the instantaneous elastic strain $\varepsilon_e$, is also shown in Table 3.

The coefficient of the Prony series that represents the short-term creep curves, shown in Tables 3 and 4, were used to calculate the coefficient of the following series equation predicting the long-term creep at 21.1 MPa:

$$D(t) = \varepsilon_e^{21.1} + D_1^{24.6}\left(1 - e^{\frac{-t}{48}}\right) + rD_1^{20}\left(1 - e^{\frac{-t}{400}}\right) + rD_1^{28}\left(1 - e^{\frac{-t}{4000}}\right) \quad (14)$$

Where $\varepsilon_e^{21.1}$ and $D_1^{21.1}$ are the coefficient of the Prony series equation that represent the 21.1 MPa short-term creep curve. The last two terms of Eq. (14), which constitute the prediction terms, are determined from the results of the short-term creep tests performed at elevated axial stresses, 24.6 and 28 MPa.

Coefficient $D_1^{24.6}$ and $D_1^{28}$ are the coefficients that correspond to the 24.6 and 28 MPa short-term creep curve, respectively. The factor $r$ is used to adjust the coefficient so that the error in the predicted creep may be minimized. Different values of $r$ were substitute in Eq. (14) in order to define the range of $r$ for which the error is minimized. A single value of $r$ does not minimize the error of the predicted creep strain in all specimens. We determined the value of $r$ to minimize the error of the results of the short-term creep tests performed at 24.6 and 28 MPa.

**Table 4** The coefficient of Pony series for short-term tests

| sample | $r$ | $\varepsilon_e^{21.1}$ | $D_1^{21.1}$ | $rD_1^{24.6}$ | $rD_1^{28}$ |
|---|---|---|---|---|---|
| A | 1.88 | 53,797 | 248.374 | 484.788 | 523.452 |
| B | 1.87 | 53,541 | 191.585 | 393.459 | 423.042 |
| C | 1.91 | 53,402 | 142.382 | 287.053 | 296.118 |

It was observed that the values of $r$ for which the error was minimized could be related to the ratio of the Prony series coefficients and the average creep factor of all stresses $f_{ave}$ by

$$r = \frac{D_1^{21.1}}{D_1^{24.6}} + \frac{D_1^{24.6}}{D_1^{28}} - f_{ave} \quad (15)$$

Where $D_1^{21.1}$, $D_1^{24.6}$, $D_1^{28}$, and $f_{ave}$ are listed in Table 4. The ratios of the coefficient in Eq. (15) represent the strain curve. The ratio $D_1^{21.1}$ to $D_1^{24.6}$, for example, the ratio of the slopes of the 15 MPa curve and the 24.6 MPa at $t$=48. This can be proved by using the first derivatives of Eqs. (5) and (6), which represent the 21.1 and the 24.6 MPa short-term creep strain curves. The values of $r$ shown in Table 4 were determined by Eq. (15).

The values of $r$, determined by Eq. (15), and other coefficients of Eq. (14) display the coefficient of different Prony series equation. The Prony series equation that predict the compressive long-term creep strain of sample 1, for example, is constructed by using values listed in the first row, as follow:

$$D(t) = 5,3797 + 248.374\left(1 - e^{\frac{-t}{48}}\right) + 484.788\left(1 - e^{\frac{-t}{400}}\right) + 523.452\left(1 - e^{\frac{-t}{4000}}\right) \quad (16)$$

Two Prony series equations, similar to Eq. (16), were developed to predict the long-term strain creeps.

## Evaluation of the short-term creep test

The predicted and the experimental creep strain curves are shown in Fig 3; the deference between the predicted and the experimental creep strain curves are because of the instantaneous elastic strain, heterogenetic and anisotropic properties of grouting samples ,and the inaccuracy of the

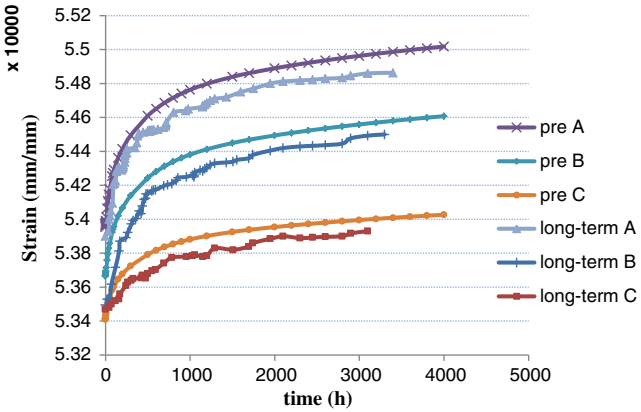


**Fig 3** Predicted and long-term measured creep strain curve

prediction method. The inaccuracy of the prediction method was isolated by subtracting the instantaneous elastic strain from both the predicted and experimental creep strain values.

A more accurate evaluation is made by a quantitative comparison of the results. The predicted specific creep and creep strain values are compared with the corresponding experimental values obtain from a long-term creep test (Table 5). The difference between the predicted and experimental values is expressed as a percentage of the experimental values.

The maximum error of the predicted creep compliance values shown in Fig. 3, is less than 7.1 % for all samples. The minor difference between the predicted and the experimental creep strains indicate that the short-term creep tests can be successfully used to predict the long-term creep deformation of the grouting resin samples examined.

## Effect of stress ratio

The rate of strain and the value of strain at any particular time depend upon the relative level of stress in relation to the yield limit of the specimens (Lama and Vutukuri 1978). It was observed that the coefficient of the exponential terms in Eqs. (5–7) increased with stress, see Table 3. As expected, a higher stress ratio resulted in a lager creep strain. However, in comparison with the stress ratio results, the creep strain is not proportional to the rate of axial stress increase, but to the deviator of stress (i.e., $\sigma_1$–$\sigma_3$).

**Table 5** Maximum differences between predicted and experimental creep

| samples | Creep strain | | |
|---|---|---|---|
| | Prediction (μ) | Experimental (μ) | Error (%) |
| A | 53,990 | 53,882 | 0.20 |
| B | 53,771 | 53,425 | 0.65 |
| C | 53,410 | 53,471 | −0.11 |

In the creep strain predicted, more than 20 % of the final creep took place within the first 40 h and nearly 50 % during the first 200 h, as shown in Fig 3. In the long-term creep strain, however, 20 % of final creep was measured within first 71 h and 50 % during the 231 h.

## Effect of confining pressure

Mollamahmutoglu (1999) conducted creep test on grouted sand specimen and found that increase in differential stress increased the creep rate considerably. It was observed that an increase in confining pressure somewhat decreased creep rate. In general, it is found that the effect of confining pressure is to decrease creep rates, increase static fatigue failure time, and increase the amount of inelastic deformation the rock can sustain before failure. It was observed that the coefficient of the exponential terms in Eq. (14) decreased with increasing confining pressure, see Tables 3 and 4.

According to several studies done on the rock samples, the creep rate of a specimen directly depends on the deviator of stress (i.e. $\sigma_1$–$\sigma_3$) applied to the central. Confined core of the specimen and preliminary indications show that it is independent of the magnitude of either the major principle stresses (Buavari, 1982). However, in this paper, different confining pressures were used to predict time-dependent behavior of the grouting material in deferent stress condition (i.e., $\sigma_1$–$\sigma_3$). It has been concluded that by increasing confining pressure due to high expansion of the grouting material, the time-dependent strength of the support system (grouting bolt) will be increased. It is worth mentioning that the creep rate of a grouting material specimen directly depends on the deviator of stress (i.e. $\sigma_1$–$\sigma_3$).

## Conclusions

In short-term triaxial tests on the grouting material carried out to predict long-term creep behavior in different axial and confining stress.

The following conclusions are drawn:

1. The long-term tests creep prediction models are formulated to facilitate an understanding of the behavior of the grouting material through the long-term creep strain is negligible, as less as 7.1 %.
2. The creep strain grows rather fast at early ages. More than 20 % of long-term creep took place within the first 71 h and nearly 50 % during the first 231 h.
3. As expected, a higher stress ratio resulted in a lager creep strain. However, in comparison with the stress ratio results, the creep strain is not proportional to the rate of stress increase. It was observed that the coefficient of the

exponential terms in prediction formula increased with stress.

4. In general, according to the previous studies, it has been found that the effect of confining pressure is to decrease creep rates. Given the experimental investigation, by using certain amount of expanding material mixed in grouting which leads to increase confining pressure on grouting and rock bolts due to expansion, long-term stability of the support system increases. It is worth mentioning that the creep rate of a grouting material specimen is directly depends on the deviator of stress (i.e., $\sigma_1$–$\sigma_3$).
5. Transient creep for the multiple stress levels tests can be well described by a power function of time.

**Acknowledgment** The writers gratefully acknowledge the test facilities and measurement data for this work, which was supported by the School of Mining Engineering and the Mining Research Center of University of New South Wales, Sydney, Australia. The authors would like to thank Prof. J. Galvin, Prof. B. Hebel White, and Dr. B. Lin for their assistance and providing valuable data.

## References

ASTM D 4543 (Reapproved 1991) Standard practices for preparing rock core specimens and determining dimensional and shape tolerances. Annual book of ASTM standards, Section 4, construction, Soil and Rock , Building Stones, Conshohocken, PA: American Society for testing and Materials, Vol. 04.08

Atkinson BK (1975) Experimental deformation of polycrystalline pyrite: effects of temperature, confining pressure, strain rate, and porosity. Economic Geology 70:473–487

Boidy E, Bouvard A, Pellet F (2002) Back analysis of time-dependent behavior of a test gallery in claystone. Tunn Undergr Sp Tech 17:415–425

Jo BW, Ta GH, Chang HK (2007) Uniaxial creep behavior and recycled-PET polymer concrete. Constr Build Mater 21:1552–1559

Barla G (2001) Tunneling under squeezing conditions. In: Tunneling Mechanics, Eurosummerschool, Innsbruck., pp 169–268

Buavari S (1982) Fundamental principles of solid mechanics. L HL&H Mining Timber: 30–55

Celtite catalogue, Australian manufacturer of strata control products for supply to the mining, civil engineering and tunneling industries.

Cruden DM (1971) The form of the creep law for rock under uniaxial compression. Int J Rock Mech Min Sci. 11:129–156

Charalambous K) 1991) Accelerated compression and flexural creep testing of polymer concrete. PH.D Dissertation, University of Texas at Austin

Chen T (2000) Determining a Prony Series for a viscoelastic material from time varying strain data. U.S. Army Research Laboratory, Hampton

Dusseault MB, Fordham CJ (1993) Time-dependent behavior of rocks. In: Hudson JA (ed) Comprehensive rock engineering, principles, practice and project, 3rd edn. Pergamon Press, Oxford, pp 119–149

Ghorbani M, Sharifzadeh M (2009) Long-term stability assessment of Siah Bisheh powerhouse cavern based on displacement back analysis method. Tunn Undergr Sp Tech 24:574–583

Hobst L, Zajíc J (1983) Anchoring in rock and soil. Developments in geotechnical engineering, 2nd edn. Elsevier, New York. ISBN 0444600779

Heap M, Baud P, Meredith P (2008) The influence of effective stress and pore fluid pressure on brittle creep in water-saturated darley dale sandstone. Geophysical Research Abstracts 10, EGU2008-A-00263

Jaeger JC, Cook NGW (1979) Fundamental of rock mechanics, 3rd edn. Chapman & Hall, London, pp 79–311

Kranz RL (1980) The effects of confining pressure and stress difference on static fatigue of granite. Journal of Geophysical Research: Solid Earth 85(B4):1854–1866. doi:10.1029/JB085iB04p01854

LeComte P (1965) Creep in rock salt. J Geol 73:469–484

Lockner D, Byerlee J (1977) Acoustic emission and creep in rock at high confining pressure and differential stress. Bull Seismol Soc Am 67(2):247–258

Lama RD, Vutukuri VS (1978) Handbook on Mechanical Properties of Rocks, 2nd edn. Trans Tech Publications, Clausthal

Mollamahmutoglu M (1999) Effect of incremental loading on the creep behavior of chemically grouted sand. Bull Eng Geol Environ 57:353–358

Nadimi S, Shahriar K, Sharifzadeh M, Moarefvand P (2010) Triaxial creep tests and back analysis of time-dependent behavior of Siah-Bisheh cavern by 3-dimensional distinct element method. Tunn Undergr Sp Tech. 26(1):155–162

OilAir Hydraulics Inc. catalogue (1996) Accumulator Training Manual, October

Ping X, Xilun X (1996) Experimental study on creep characteristics of granite of the TGP. Chin. J. Geotech. Eng. 8(4):63–67

Soleiman DM, Shahriar K, Moarefvand P, Gharouninik M (2011) Application of the strain energy to estimate the rock load in squeezing ground condition of Eamzade Hashem tunnel in Iran. AJGS Journal. doi:10.1007/s12517-011-0117-1

Zarei H, Sharifzadeh M (2010) Identifying geological hazard related to tunneling in carbonate karstic rocks - Zagros. Iran AJGS Journal doi:10.1007/s12517-010-0218-y

Wawersik WR, Zimmerer DJ (1994) Triaxial creep measurement on rock salt from the jennings dome, Louisiana, borehole LA, core #8. Geomechanics department 6117, Sandia National Laboratories, Albuquerque. doi:10.2172/10181963

Yongsheng Z, Changrong H (2005) An experimental study of quartz-coesite transition at differential stress. Chin Sci Bull 50:446–451

Zhang LQ, Yue ZQ, Yang ZF, Qi JX, Liu FC (2006) A displacement-based back analysis method for rock mass modulus and horizontal in situ stress in tunneling—illustrated with a case study. Tunn Undergr Sp Tech. 21(6):639–649